Validating engineering objectives of hydraulic fracture stimulations using microseismicity

Ted Urbancic[1] and Adam Baig[1*] describe how engineering objectives of hydraulic fractures can be identified and validated through source characterization of microseismicity recorded as part of the stimulation programme.

Microseismic monitoring is routinely being used to identify overall hydraulic fracture characteristics such as geometry, half width, stage overlap, and estimated stimulated reservoir volume. Engineers utilize these data along with injection and production data to assess the effectiveness of a stimulation programme However, microseismic event locations by themselves do not answer well the questions on improved reservoir drainage which will ultimately control the increases in production.

As each microseismic event can be related to shear-tensile failure on a fracture plane, and each fracture plane is part of a discrete fracture network (DFN), using the microseismic data to reconstruct the DFN activated by the stimulation will enable the use of these data to answer these next higher-order questions on the effectiveness of the stimulation. In this paper, we illustrate with two case studies how, under multi-well downhole monitoring efforts, these questions can be addressed.

Inherently, microseismic signals contain information about the physical processes at the source (event origin). By utilizing techniques such as seismic moment tensor inversion (SMTI) analysis (Baig and Urbancic, 2010), additional source characteristics such as the principal strain axes, failure mechanisms, and potential fracture plane orientations can be determined. Combining this processing stream with an accurate measurement of microseismic source parameters, such as source radius, allows for an accurate description of the activated DFN.

Solving for SMTI derived parameters is not trivial and numerous papers have been written discussing various approaches, models, and methods of assessment of validity. All approaches require that the events being examined are sufficiently surrounded by a three dimensional network of measuring points (network of sensors). For hydraulic fracture stimulations, access in many cases restricts the coverage; however, multi-well array configurations can provide sufficient coverage, as determined through condition number analyses, to solve for the failure components of individual events.

The DFN interpretation of a microseismic event cloud is a cornerstone towards the incorporation of microseismic data into geomechanical modelling. The orientations of the activated fractures offer a direct validation of whether the fracture design objectives of targeting one fracture set over another.

For example, an approach being investigated by numerous producers, referred to as hesitation stimulations, in theory can be used to create a dendritic (branching) fracture network to enhance well productivity (up to two to five times over conventional fracturing) and to rapidly drain the reservoir around a wellbore as compared to bi-wing fractures (Kiel, 1977). The process uses a cyclic injection procedure by shutting the well in or allowing it to flow back, and then resuming injection to open secondary fractures offset from the initial primary fracture orientation. Similarly, changes in injection pressure rates, the number of perforations, and slurry rates may result in variations in local stress conditions that potentially can affect the type of fracturing, the fracture intensity, and overall fracture complexity associated with a particular stimulation programme.

The DFN fracture lengths can be examined in terms of their scaling processes. Fractures occur in rock according to a fractal distribution, whereby the distribution of fracture lengths can be described in terms of a power law. Knowledge of this distribution is a critical input for numerical simulations of reservoir performance. The size scales of the activated fractures as inferred from the microseismic data allow for this power law to be extended further, bridging the gaps in the fracture size distributions between curvature features in 3D seismic to the outcrop scale.

Extending further the SMTI-derived DFN, the stimulated fracture network can be examined in the context of a stimulated reservoir volume (SRV). Estimates of SRVs have evolved over the lifetime of the technology. Early attempts to define SRV by using envelope functions around microseismic event distributions generally results in large overestimates of the stimulated zone due to the over-emphasis that outlier events can have on the calculation and/or the inability to distinguish between fluid induced versus stress induced events. Refinements to distill the SRV down to the most seismically deformed volume reduces the emphasis on the furthest-out events but still does not incorporate any information on the failure mechanisms or the fracture sets being activated. By considering the fracture

[1] *ESG Solutions.*

[*] *Corresponding author, E-mail: adam.baig@esgsolutions.com*

intensity (FI), the aggregate fracture length per unit area in the reservoir, the concept of stimulated surface area can be examined. Furthermore, these stimulated fractures can form a number of intersections, which leads to the concept of fracture complexity (FC). The stimulated volume can then be interpreted in terms of fracture complexity.

Another consideration to the stimulated reservoir volume is then a determination of where fracture complexity allows for a part of the reservoir to be well connected back to the perforations. Finally, high-quality events can be inverted for a general solution, which admits a volumetric component to the solutions, implying that there is an opening component to many of these activated mixed-mode shear-tensile failures. With reference to a geomechanical model, and using the focal mechanism in conjunction with the source radius, an aperture for each event can be inferred, and the amount of net opening for a voxel in the reservoir can be determined. This enhanced fluid flow (EFF) volume of the reservoir then translates to another consideration in the overall stimulated reservoir volume.

In this paper, we focus on one aspect of validating engineering design by examining microseismicity in the context of an activated DFN associated with a stimulation designed to increase fracture complexity in a naturally fractured shale formation. In addition to event locations, multi-array and multi-well configurations were deployed which allowed for the assessment of general moment tensor solutions for the observed events. This provided an opportunity to examine the relative spatial and temporal behaviour of fracture orientations (azimuths and dips) as a function of the stimulation programme. Based on these analyses, we discuss how augmenting observations of microseismicity with moment tensor derived fracture data can be used to assess the effectiveness of different fracture stimulation programmes to increase fracture complexity. In particular, our analysis considers how the impact of changing the number of perforations, injection pressure rate changes, and fracture hesitation approaches can be used to optimize the engineering (stimulation) design.

In a second example, we consider how the fracture size distributions for the stimulation, including the interactions and overlap between different stages, and the FI, FC and EFF, can be used to interpret the stimulated reservoir volume; in this case, in the context of a zipper-frac completion of an entire pad. The development of these fields over the whole completion illustrates how the interaction and overlapping event distributions are critical in the development of SRV in the reservoir.

Case study 1: Validating engineering approaches to increase fracture complexity

Our analysis is focused on examining the stimulations associated with two long horizontal wells in naturally fractured shale. Three arrays were deployed consisting of a minimum of 16–24 triaxial 15Hz omni-directional geophones magnetically clamped in a vertical observation well along with at least two additional 24-level multi-point arrays in the vertical and horizontal sections of nearby wells. Based on the condition number analysis as outlined by Urbancic et al. (2010), the arrays were positioned in order to meet the prerequisites for obtaining general solutions.

General solutions with low condition numbers were used in the determination fracture orientations, utilizing an approach similar to that proposed by Gephart and Forsyth (1984). Only stable general and double couple solutions were retained for further analysis. Overall, our analysis considers ~6200 events for 10 stages of the stimulation (See Figure 1).

The stimulation program consisted of different approaches. In Well 1, with the exception of Stage E, the stages consisted of at least four perforations, whereas a more varied programme was considered for Well 2, consisting of three and four perforation stages as well as two stages that included hesitation intervals of a few hours and over one day.

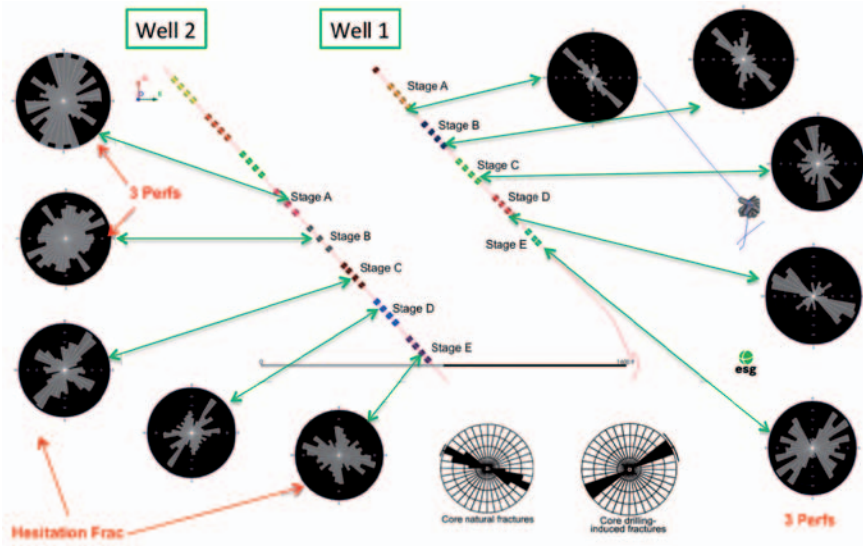

Figure 1 *Plan view of well locations along with the rosette diagrams for the SMTI derived fractures for each stage. Additionally, the mapped natural and induced (secondary) fractures described by Gale et al. (2007) are also shown on rosette diagrams. Unless indicated, each stage consisted of four perforations. North direction is towards the top of the figure.*

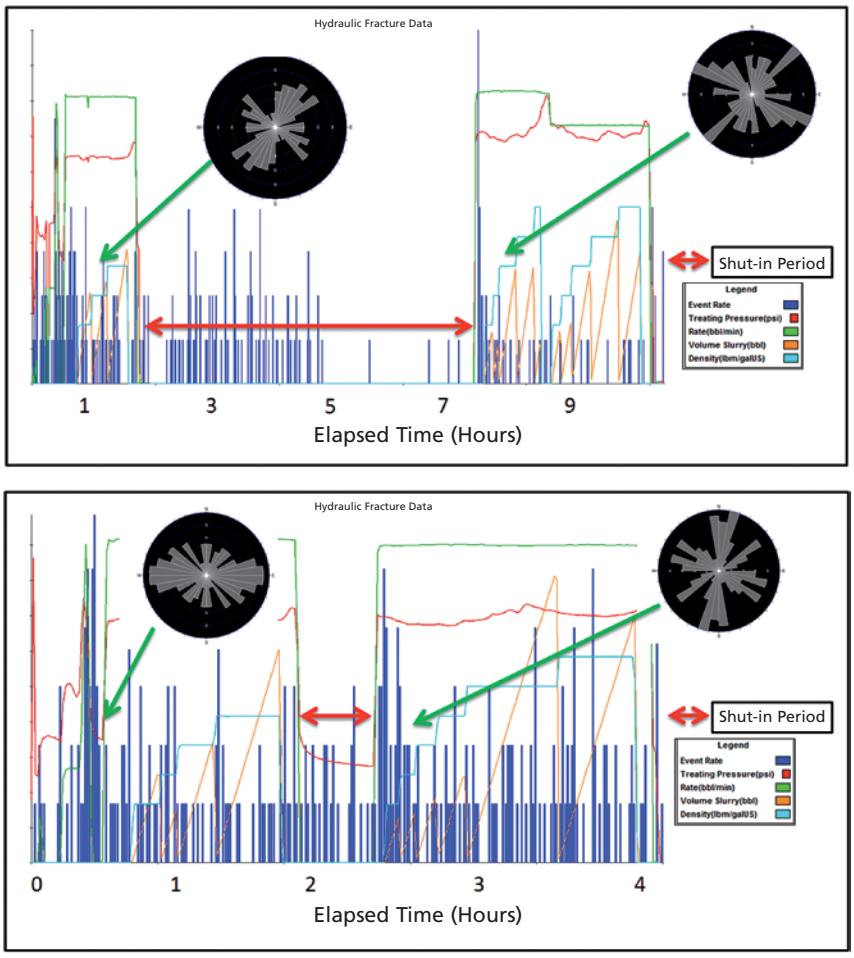

Figure 2 *Top. Well 2, Stage C hesitation fracture with an extended shut-in period. Bottom. Well 2, Stage E hesitation fracture with a shortened shut-in period.*

Included in Figure 1 are rosette diagrams showing the orientation of SMTI-derived fractures with dips greater than 60^0. (Note: over 90% of the observed events were associated with steeply dipping fractures). Also included on Figure 1 are the fracture orientations mapped from core just to the south of the study area (Gale et al., 2007). These fractures can be classified into two groupings, those referred to as natural fractures developed during paleo-stress conditions and those induced by core drilling (secondary fractures) developed under the current stress regime. Generally, the natural fractures trend NW–SE and are steeply dipping whereas the induced fractures are steeply dipping to the NE–SW.

In general, the observed fracturing for the early Well 1 stages are dominated by fractures similar to the mapped natural fracture network. Observed differences between the mapped and derived fracture orientations are likely related to a slight re-orientation of the regional stress field between the data collection sites. However, the observed consistency in orientation suggests that the stimulation has activated the pre-existing natural fracture network. Stages A to D in Well 1 all exhibit primarily NW–SE trending fractures. These stages were completed based on utilizing four perforations.

In contrast, Stage D in Well 2, also a four-perforation stage, the fracture network appears to be dominated by activated secondary fractures and to smaller degree natural fractures. These differences are possibly due to the proximity of the stages to nearby or previously fractured areas and thereby the observed fracture network is likely related to local re-orientation of the stress field. For Well 1, Stage E, three perforations were used and interestingly, the observed fractures are widely distributed, resembling a 'starburst' pattern. This is very similar to what was observed for Stages A and B for Well 2, also three perforation stages. It appears that stages with fewer perforations resulted in starburst fracturing and a significant increase in associated fracture complexity.

Similar in concept are the hesitation fracture stages in Well 2 (Figure 2: Stages C and E). The hesitation stimulation programmes were effectively the same, with the exception of the duration of the flow back time associated with the cyclic injection. In either case, the hesitation approaches resulted in observed differences in fracture orientations prior to and post the flow back interval. Prior to flow back, activated fractures were dominated by singular fracture sets, either trending ~E–W or NE-–SW. Following the flow back interval,

activated fractures include the initial pre-flow back fracture set and a dominant secondary fracture set. Based on these observations we can speculate that local re-orientation of the stress field as a result of the pre-flow stimulation allowed for the activation of a secondary fracture set. The continued activation of the initial fracture sets suggests that differences in failure mechanisms may be occurring, where previously opened fractures are exhibiting closure. In both cases, the level of fracture complexity has increased as a result of the hesitation process. In the future, the effectiveness of the created transport network is to be examined as part of a study of the failure mechanisms.

Case Study 2: Zipper-frac completion highlights the development of a stimulated DFN

In the second case study, we build on the discussion from the first example by considering the development of a DFN over two multiple-well zipper-frac shale completions in NE British Columbia, Canada. The completions were monitored from a number of different configurations, such that treatment wells could be temporarily re-purposed as observation wells when not being pumped. But generally the geophone arrays were deployed in a multi-well geometry around the treatment zone. This was in order to obtain a sufficiently wide distribution of angles of sensors around the treatment zone as shown through the condition number analysis discussed in the previous example. The monitoring arrays consisted of triaxial, omni-directional, 15 Hz sensors with 12–48 levels with magnetic clamping.

Initial processing of the data resulted in over 200,000 events of various qualities. We focus on the highest quality dataset, as shown in Figure 3 for one of the pads, where the events had clear (SNR>3) *P* and *S* phases.

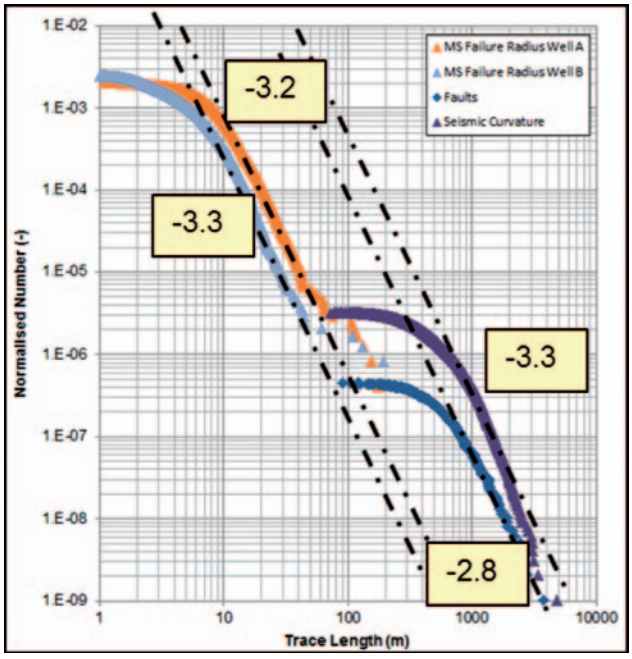

Figure 4 *Fracture length distributions as estimated from nearby mapped faults (blue), seismic curvature features (purple), and two microseismic datasets (orange and grey). The slopes of the distribution describes the power law necessary to incorporate fracture lengths into geomechanical models. Figure reproduced from von Lunen (2012).*

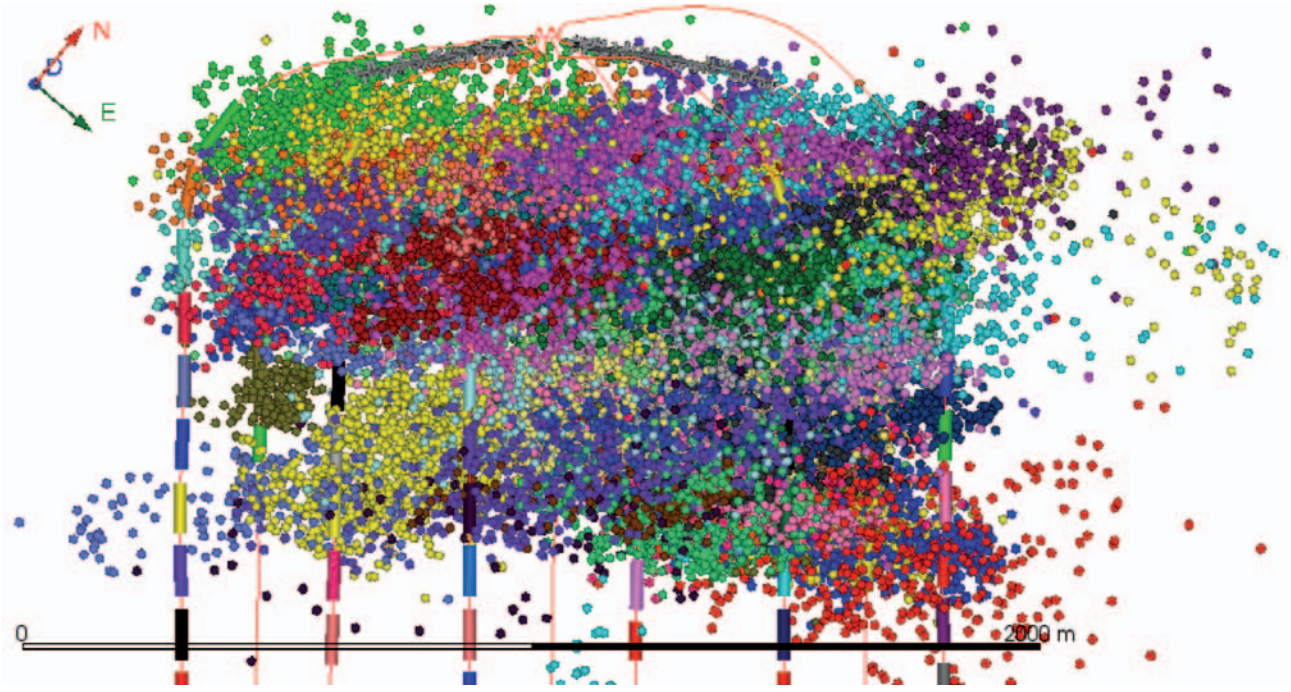

Figure 3 *Plan view image of over 40,000 higher quality events recorded from a zipper frac in the Horn River Basin in NE British Columbia. Because the events are coloured by stage, the overlapping nature of the events is apparent.*

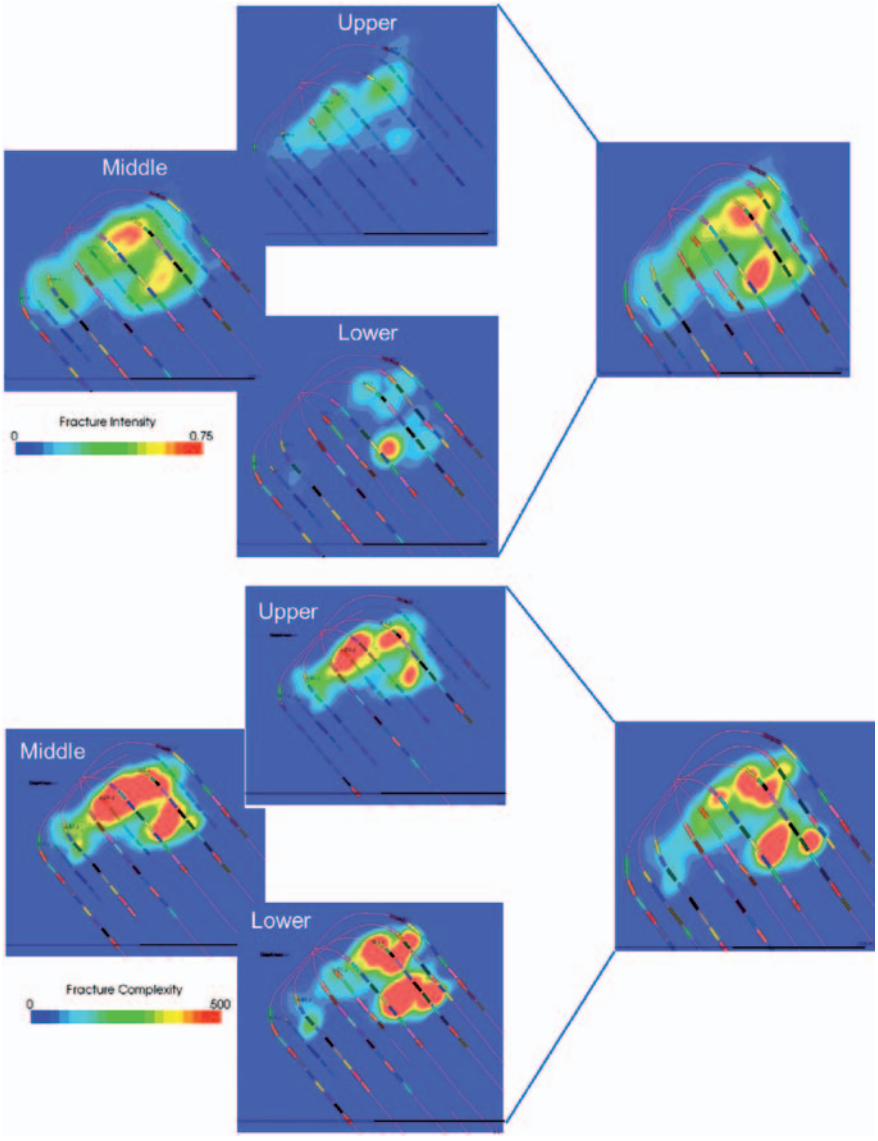

Figure 5 *(above) Fracture intensity (FI) in the upper, middle and lower formations in the reservoir then synthesized into the total FI for the reservoir. (below) Fracture complexity (FC) presented in the same fashion.*

Although the treatment wells were drilled to target different lithological intervals, the event distributions generally transitioned these lithological boundaries and showed a high degree of overlap. One baseline question is how does this overlap impact SRV? Are differently oriented opening fractures enhancing FC and EFF in these regions? Or do these fractures represent closures of previously opened fractures, negatively impacting the stimulation?

The size scales of the DFN were examined using the source radius as determined though a spectral examination of each event. Using a Brune (1970, 1971) model of a penny-shaped crack modified for shear-tensile failures (Walter and Brune, 1993), the corner frequency of an event is defined as being inversely proportional to the radius of the crack. In Figure 4, we present a comparison of the size scales of the microseismic events, compared with the size scales of fracture sizes as estimated from 3D seismic curvature features and known fault features in the reservoir. The microseismic datasets are not seeing in absolute terms the same number of fractures, as indicated by the horizontal detachment between these datasets and the curvature and fault datasets, but the slopes of the distributions are in very good agreement. They also provide information at a different size scale as compared to the curvature data, filling in gaps in the overall power law distribution.

The spatial distribution of fractures in the DFN leads to using this distribution to better determine stimulated reservoir volumes due to the treatment. In Figure 5, we illustrate the concepts of FI and FC with the dataset shown in Figure 3. The data are divided over the three treatment intervals to illustrate that, despite the overlap and transitioning of events across formation boundaries, there are areas in the treatment that are more efficiently activated than other

areas. The FI indicates that the fracturing is most active in the middle formation, with a localized patch of increased FI in the lower formation. While the FI plots indicate how much of the fracture network is being activated in each of the formations, the fracture complexity for the same dataset shows that the areas which will have the best drainage potential, forming the most interconnected fractures, is not necessarily in a one-to-one relationship with FI. FC for the upper formation, for example, indicates that the fracturing pattern here is complex even where FI is indicating that a more modest amount of fractures are being activated.

Completing the picture, in terms of stimulated reservoir volume is the EFF, which incorporates the fracture opening components into the estimates for SRV under the assumption that where the opening mechanisms are, in relation to the increased FI and/or FC, is where the greatest production will occur. Figure 6 shows the development of the EFF as a number of different stages are being frac'ed. The initial EFF field for the one stage is showing that the opening component events (enclosed by the isosurface) are relatively isolated from one-another from the one stage. The next stage, which overprints the initial stage activates the same area, and acts to connect together these pockets of EFF. We show on the left side of the figure the effect that four consecutive stages have on connecting together a core of EFF for the region that they all overlap. Over the whole completion, the EFF for the entire treatment is contained in a volume that is well-connected within itself, although there are still event outliers. These outliers, as seen during the growth of the SRV, are likely events responding to stress transfer from the treatment volume rather than representing any fluid connectivity, themselves.

Conclusions

In this paper, we have shown how engineering objectives of hydraulic fractures can be identified and validated through source characterization of microseismicity recorded as part of the stimulation programme. In particular, by utilizing SMTI approaches we can address engineering objectives such as obtaining good estimates of fracture orientation, fracture extent, and fracture growth both near the treatment well as well as fracture extension regions away from treatment zones, defining the DFN, FC, and FI, establishing the power law distribution of fracture lengths, identifying regions of EFF for realistic estimates of stimulated reservoir volume, and utilizing this information to validate reservoir models for the purposes of reserve estimation.

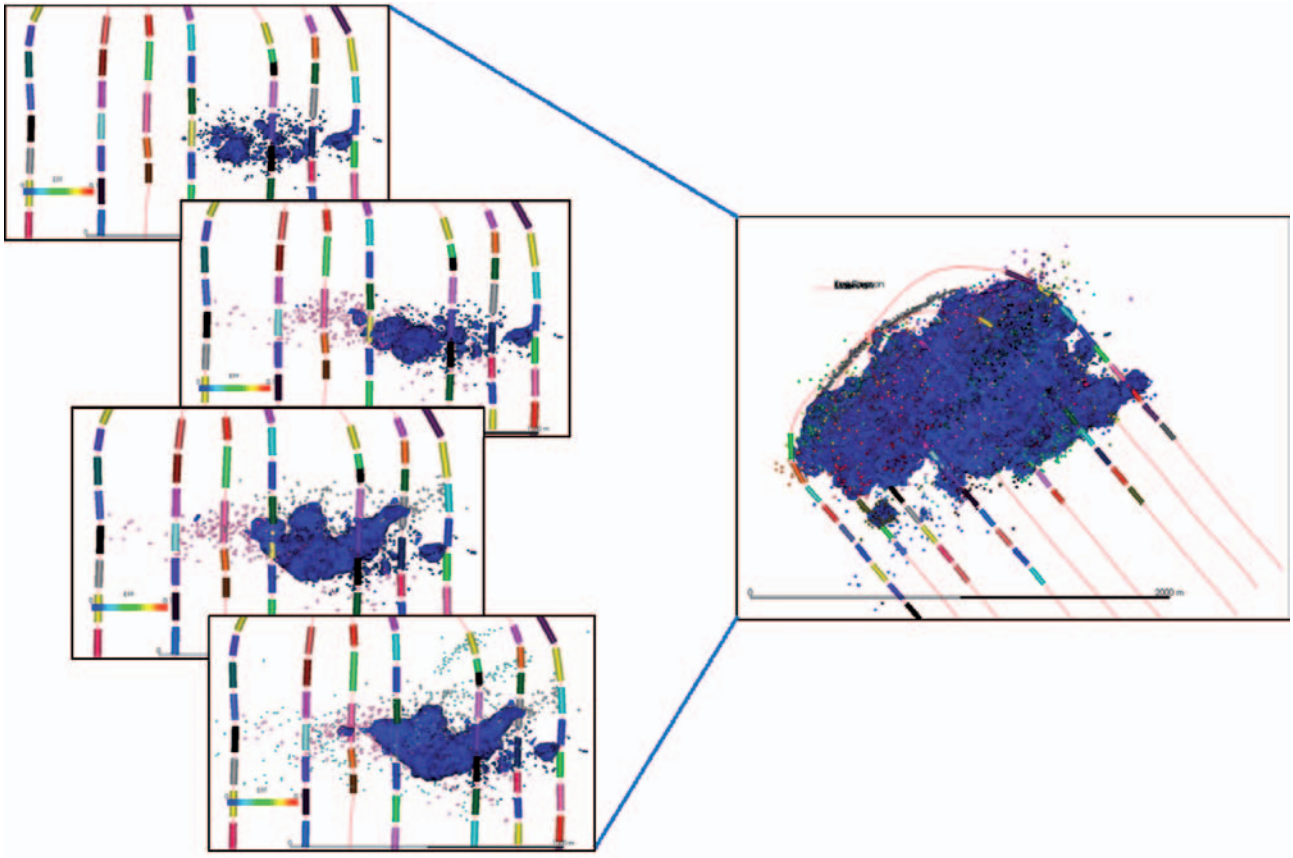

Figure 6 *(left) Enhanced fluid flow (EFF) field, as represented by an isosurface, evolves over four overlapping stages to connect initially isolated compartments of opening events together into a core of enhances fluid flow characteristics. (right) the total EFF field for the SMTI events monitored during the completion. Note that the figures on the left are rotated with respect to the total EFF figure for display purposes.*

Two case studies associated with stimulation of naturally fractured shale formations were discussed and used to emphasize how different fracture sets are activated by differences in the stimulation programme. We identified how changing the number of perforations and the cyclic hesitation style of stimulation can result in increased FC with starburst fracturing or with the activation of secondary pre-existing fractures formed under either the current or paleo-stress regimes. These observations suggest that the engineering objectives of the stimulation programme can be met or potentially varied and used to control stimulation effectiveness.

Further, we showed that SMTI-derived fracture planes could be used to define the distribution of the size-scales of fractures in the form of a power law; this provides a direct input to constraining and validating reservoir models. Most interesting, these size scales, together with the fracture orientations, comprise a DFN that can be used to identify the FC and FI that potentially identify favourable pathways for improved drainage in the reservoir. As well, utilizing the concept of EFF can refine estimates of SRV objective. In summary, our analyses suggest that a detailed analysis of microseismic waveforms provides an opportunity to identify engineering objectives and assess/validate the effectiveness of different stimulation designs.

References

Baig, A. M. and Urbancic T.I., 2010, Microseismic moment tensors: A path to understanding frac growth. *The Leading Edge*, **29**, 320–324.

Brune, J. N. [1970] Tectonic Stress and the spectra of seismic shear waves from tectonic earthquakes. *J. Geophys. Res.*, **75**, 4997–5009.

Brune, J. N. [1971] Correction. J. *Geophys. Res*, **76**, 5002.

Gale, J. F. W., Reed, R. M. and Holder, J. [2007], Natural fractures in the Barnett Shale and their importance for hydraulic fracture treatments, *AAPG Bull.*, **91**, 603–622.

Gephart, J. and D. Forsyth [1984] An improved method for determining the regional stress tensor using earthquake focal mechanism data: An application to the San Fernando earthquake sequence. *Journal of Geophysical Research*, **89**, 9305–932.

Kiel, O. M. [1977] The Kiel process reservoir stimulation by dendritic fracturing. *SPE 6984-MS.*

Von Lunen, E. [2012] Utilizing Geophysical Concepts in Unconventional Resource Assessment of Shale Gas. *SEG Development and Production Luncheon.*

Urbancic, T. I., Baig, A. M., Guest, A. and Buckingham, K. [2010] HFM: Dynamic Behavior of Fracture Networks. *SEG Microseismic Workshop*.

Walter, W. R. and Brune, J. N. [1993] Seismic spectra from a tensile crack. J. Geophys. Res., 98, 4449–4459.